An Automated and High Precision Quantitative Analysis of the ACR Phantom

P. J. Markiewicz, Casper da Costa-Luis, J. Dickson, A. Barnes, G.Krokos, J. MacKewn, T. Clark, C. Wimberley, G. MacNaught, M. M. Yaqub, J. D. Gispert, B. F. Hutton, P. Marsden, A. Hammers, A. J. Reader, S. Ourselin, K. Herholz, J. C. Matthews* and F. Barkhof*

***Abstract*—A novel phantom-imaging platform for automated and high precision imaging of the American College of Radiology (ACR) PET phantom is proposed. The platform facilitates the generation of an accurate μ-map for PET/MR systems with a robust alignment based on two-stage image registration using specifically designed PET templates. The automated analysis of PET images uses a set of granular composite volume of interest (VOI) templates in a 0.5 mm resolution grid for sampling of the system response to the insert step functions. The impact of the activity outside the field of view (FOV) was evaluated using two acquisitions of 30 minutes each, with and without the activity outside the FOV. Iterative image reconstruction was employed with and without modelled shift-invariant point spread function (PSF) and varying ordered subsets expectation maximisation (OSEM) iterations. Uncertainty analysis of all image-derived statistics was performed using bootstrap resampling of the list-mode data. We found that the activity outside the FOV can adversely affect the imaging planes close to the edge of the axial FOV, reducing the contrast, background uniformity and overall quantitative accuracy. The PSF had a positive impact on contrast recovery (although it slows convergence). The proposed platform may be helpful in a more informative evaluation of PET systems and image reconstruction methods.**

I. Introduction

Phantoms are test objects that provide an accurate means of performing calibration as well as evaluation of performance of imaging systems such as positron emission tomography (PET) [1]. Phantom imaging proved helpful in standardisation and assessment of the reproducibility and variability of PET quantitative performance for multi-centre clinical studies [2] as well as in investigation of the impact of image protocols, including image reconstruction methods [3]. The Jaszczak ACR PET phantom was used in this work as it offers multiple tests for uniformity, noise, spatial resolution and contrast within one acquisition [2]. The novelty of the proposed open-source analysis platform lies in the vector graphics design of multiple phantom templates for robust image registration, accurate attenuation correction for PET/MR, and granular sampling of the PET system response to the step functions generated by the cylindrical inserts.

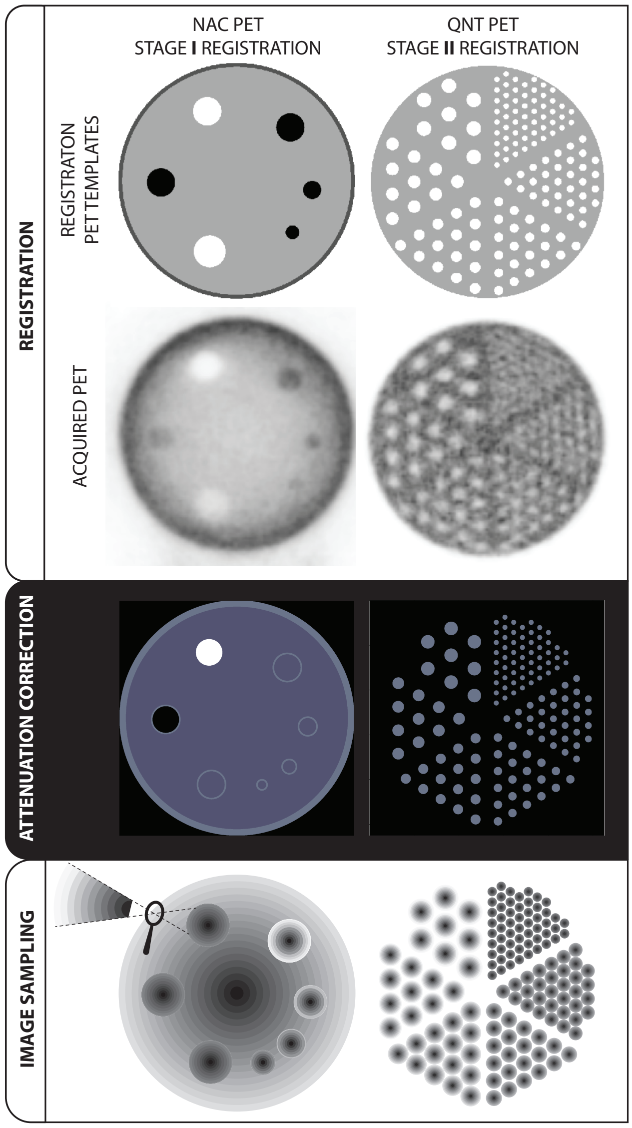

Fig. 1. Design of multi-purpose phantom templates. **Top**: Two-stage registration using NAC and QNT PET; **middle**: μ-map generation; **bottom**: high-resolution VOIs for granular sampling of quantitative PET images.

II. Methods

The exact 3D shape of the ACR Jaszczak phantom with all its inserts and screws is fully represented using a set of

* Joint senior authorship
Manuscript received December 1, 2021.
P. J. Markiewicz, Casper da Costa-Luis and F. Barkhof are with the Dep. of Medical Physics and Biomedical Engineering, CMIC, UCL, UK.

G. Krokos, J. Mackewn, A. J. Reader, A. Hammers, P. Marsden and S. Ourselin are with the School of Biomedical Engineering and Imaging Sciences; KCL; UK.

A. Barnes, J. Dickson and B .F. Hutton are with the Institute of Nuclear Medicine, UCL/H, UK.

T. Clark, C. Wimberley, G. MacNaught are with Edinburgh Imaging, University of Edinburgh, UK.

J. D. Gispert is with Barcelonaβeta Brain Research Center, Spain.

M. M. Yaqub and F. Barkhof are with Department of Radiology and Nuclear Medicine, Amsterdam UMC, Vrije Universiteit, Netherlands.

K. Herholz and J. C. Matthews are with the Division of Neuroscience & Experimental Psychology, University of Manchester, UK.

978-1-6654-2113-3/21/$31.00 ©2021 IEEE

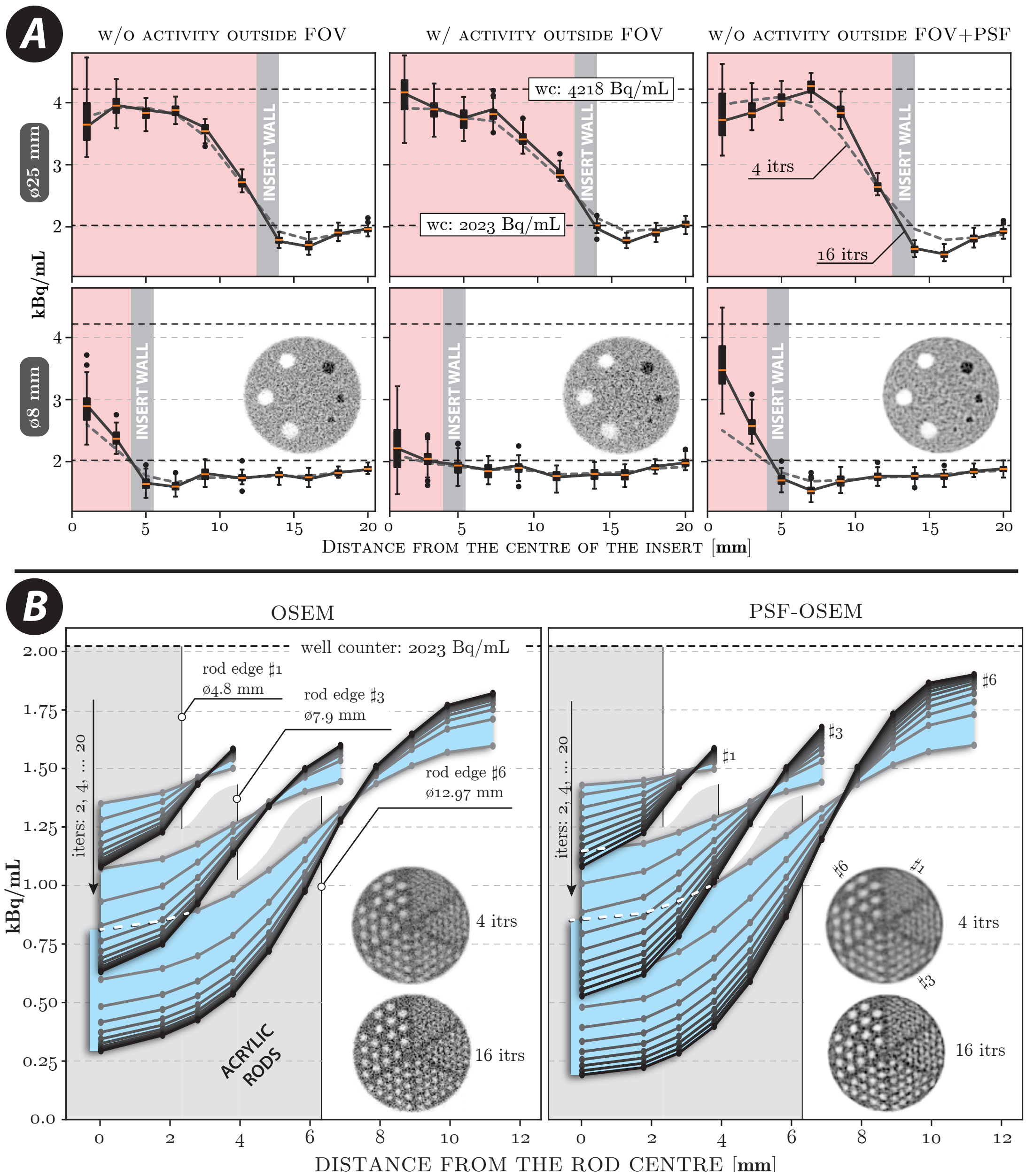

Fig. 2. Radioactivity concentration curves as the system response to the radial step function of different inserts/rods. The curves are extracted from the different PET images (without and with the activity outside the FOV, and with PSF included in reconstruction) using the VOI templates with concentric rings for hot inserts (**A**) and cold rods (**B**).

2D transaxial planes designed using vector graphics to form multiple 3D templates (Fig. 1). The robust alignment of the μ-map to the PET data is ensured using high-resolution (0.4 mm voxel size) templates for registering first the whole phantom container and the faceplate using to the non-attenuation corrected (NAC) PET, followed by registering the resolution rod template to the quantitative PET (which has better contrast for the cold rods). The advantage of this design is that the same rigid-body transformations are used for aligning the PET image sampling and the μ-map templates to the PET data, ensuring consistency between attenuation correction and image analysis. The sampling templates consist of composite VOIs of concentric rings with spacing less than 2 mm to extract the response to the radial step functions of all the cold and hot inserts using a 0.5 mm resolution grid. All image reconstruction and uncertainty analysis (using 50 bootstrap realisations of the list-mode data) was performed using Python package *NiftyPET* [4].

III. Results

The radioactivity concentration curves for two extreme hot inserts—measured by 10 concentric ring VOIs in 1 cm thick image slice—are shown in Fig. 2A. With a significant activity outside the FOV, the smallest insert is statistically indistinguishable from the background. The PSF reconstruction for both inserts yields steeper recovery of the high activity, indicating gain in image resolution at the cost of noticeable edge artefacts for the bigger insert. Valuable information is revealed when measuring the radioactivity concentration curves for the different rods (Fig. 2B)—the number of OSEM iterations not only has an effect on the image contrast but also on the image resolution (the steeper the curves, the higher the resolution). In order to benefit from the higher contrast and resolution, when including the PSF in reconstruction, the algorithm needs more OSEM iterations, particularly for the smaller diameter rods.

IV. Conclusion

The results presented demonstrate valuable information gained by using the proposed platform for automated analysis, enabling more accurate characterisation of PET systems across sites as well as quantitative evaluation of image reconstruction methods. The platform will be available as open-source.

References

[1] Ulrich EJ, *et al.* "Automated model-based quantitative analysis of phantoms with spherical inserts in FDG PET scans", *Med Phys* 2018;

[2] MacFarlane CR, *et al.* "ACR accreditation of nuclear medicine and PET imaging departments" *J Nucl Med Tech-nol* 2006

[3] Westerterp M, *et al.* "Quantification of FDG PET studies using standardised uptake values in multi-centre trials: Effectsof image reconstruction, resolution and ROI definition parameters" *Eur J Nucl Med Mol Imaging* 2007

[4] Markiewicz, *et al.*, "NiftyPET: a High-throughput Software Platform for High Quantitative Accuracy and Precision PET Imaging and Analysis.", *Neuroinformatics* 2018